A 3D-CFD-heat-transfer-based model for the microbial inactivation of pasteurized food products

Clarissa Detomi de Albuquerque, Sébastien Curet, Lionel Boillereaux

A 3D-CFD-heat-transfer-based model for the microbial inactivation of pasteurized food products

Clarissa DETOMI DE ALBUQUERQUE, Sébastien CURET, Lionel BOILLEREAUX

GEPEA - ONIRIS - (UMR CNRS 6144), Site de la Géraudière CS 82225, 44322 Nantes cedex 3, France.

Corresponding author: sebastien.curet@oniris-nantes.fr

GEPEA - ONIRIS - (UMR CNRS 6144), Site de la Géraudière CS 82225, 44322 Nantes cedex 3, France.

ABSTRACT

This study proposes to couple a 3D-CFD and heat transfer finite elements model with the microbial inactivation approach proposed by Geeraerd et al. (2000). The CFD-heat transfer model was developed using thermophysical properties for both heating fluid (water) and the processed sample (ground beef). The kinetic microbial parameters were estimated using experimental data from the inactivation of *Escherichia coli* K12 in a packaged sample. The proposed inactivation model was tested under more severe dynamic conditions than usual (heating rates from 1 to 13 °C/min). The inactivation kinetic parameters were found independent of the heating rate applied. In addition, the results reveal that the Geeraerd et al. (2000) model without shoulder is sufficient to fit the experimental data. Such a model could be beneficial in simulating microbial inactivation for food products, thus ensuring food safety by limiting, as far as possible, overtreatment.

Keywords: Microbial inactivation; Modeling; 3D-CFD; Heat transfer; Pasteurization.

Nomenclature

a, b	dimensions of the elliptical sample (mm)
C_c	critical component related to the physiological state of the cells (-)
C_P	apparent specific heat (kJ kg^{-1} K^{-1})
D_{ref}	decimal reduction time (s)
g	gravitational constant (m/s^2)
h_{air}	heat transfer coefficient of air (W m^{-2} K^{-1})
k_{max}	specific inactivation rate (s^{-1})

L	sample length (mm)
LL	maximum likelihood
n	number of experimental data points
N	microbial population (CFU /g)
N_0	initial microbial population (CFU /g)
N_{simu}	simulated microbial population (CFU /g)
N_{exp}	experimental microbial population (CFU /g)
p	number of independently adjusted parameters within the model
P	absolute pressure (Pa)
Q	volumetric heat generation term (W/m^3)
R	radius (mm)
T	temperature (°C)
T_0	initial temperature of product (°C)
T_∞	ambient temperature (°C)
t_i	simulated time (s)
T_{ref}	microbial inactivation reference temperature (°C)
$T_{cylinder\ cell}$	temperature of lateral surfaces of the cylinder (°C)
$\vec{u}$	velocity field (m/s)
u, v, w	spatial components of velocity field
V	volume of the meat sample (m^3)
x, y, z	spatial coordinates in the three dimensions (m)
z	thermal resistance constant (°C)

Greek letters

ρ	density (kg/m^3)
μ	dynamic viscosity (Pa s)
σ	standard deviation of experimental data
λ	thermal conductivity ($W\ m^{-1}\ K^{-1}$)

1. Introduction

Prediction of microbial inactivation during thermal treatment is crucial not only to ensure the safety of food products but also to avoid overtreatment (Boillereaux, Curet, Hamoud-Agha, & Simonin, 2013). Although conventional processing technologies produce safe products, they can also lead to significant changes to the sensory and nutritional attributes of foods. In

today's quality conscious world, much attention is given to producing foods that retain superior sensorial quality but must also remain safe (Bott, 2014; Stratakos & Koidis, 2015). Consequently, the determination of the microbial destruction level that a thermal treatment can deliver to a product requires both understanding of: (*i*) the heat transfer within the food product and (*ii*) the destruction kinetics of the microorganism of interest (Valdramidis et al., 2005). The necessity of such an approach is reinforced regarding the thermal heterogeneities that occur during a pasteurization process.

A reliable inactivation parameter estimation is essential for building predictive models (Chen, 2013) and is necessary to establish safe minimal cooking-cooling conditions (Marcotte, Chen, Grabowski, Ramaswamy, & Piette, 2008). The determination of these parameters has been the subject of numerous studies, either under static (Ahmed, Conner, & Huffman, 1995; Smith, Maurer, Orta-Ramirez, Ryser, & Smith, 2001) or dynamic conditions (Garre et al., 2018; Hassani, Cebrián, Mañas, Condón, & Pagán, 2006; Juneja & Marks, 2003; Valdramidis, Geeraerd, Bernaerts, & Van Impe, 2006; Valdramidis, Geeraerd, & Impe, 2007). Different models have also been proposed to describe the microbial inactivation kinetics.

Numerous studies focusing on the estimation of microbial kinetic parameters are performed in isothermal and dynamic conditions, but under ideal laboratory conditions (capillary tubes, liquid inoculum and small sample mass). In real time industrial processing, food products are often submitted to time-varying temperatures. Moreover, due to several factors affecting heat transfer, i.e. geometry, thermophysical properties or external convection, significant thermal heterogeneities can occur. In the literature, the effect of capillary tube diameters on the inactivation parameters of *E. Coli*, in solid food, was investigated from a two-dimensional heat transfer approach (Chung, Wang, & Tang, 2007).

A recent study by Garre et al., (2018) presented a mathematical model to describe the non-isothermal microbial inactivation process. The model was dedicated to *Escherichia coli* inactivation under linear heating rates of 1, 5, 15, 35 and 40 °C/min, from 35 to 70 °C. The authors developed a mathematical model taking into account the thermotolerance of the microbial cells. The model was able to describe the experimental data using a unique set of model parameters.

Another investigation, Hamoud-Agha, Curet, Simonin, & Boillereaux, (2013) proposed to estimate D_{ref} and z-value of Bigelow's (1921) equation. These parameters were estimated for *E. coli* K12 inoculated into a model food under dynamic conditions (homogeneous

temperature distribution due to a very small solid sample). These parameters were included in the Geeraerd et al., (2000) inactivation model coupled with a 3D-heat transfer model under microwaves to illustrate the resulting inactivation heterogeneity.

The literature is rich concerning CFD and heat transfer modelling dedicated to pasteurization of food products (Bhuvaneswari & Anandharamakrishnan, 2014; Cordioli, Rinaldi, Copelli, Casoli, & Barbanti, 2014; Denys, Pieters, & Dewettinck, 2003; Dimou & Yanniotis, 2011). However, except in Hamoud-Agha et al., (2013), it is rare to find these models coupled with microbial inactivation equations and even less with real products under external dynamic conditions. These elements reflect the originality of this work proposal. In this study, a 3D-CFD and heat transfer approach is coupled with the Geeraerd et al. (2000) inactivation model. External temperature conditions (heating rates from 1 to 13 °C/min) are applied to *Escherichia coli* K12 inactivation in pre-packed ground beef. Model parameters are estimated from experimental data using the Levenberg-Marquardt algorithm (Marquardt, 1963).

2. Materials and methods

2.1 Experimental section

2.1.1 Sample preparation

Raw ground beef (Beef Steak 5% fat, Charal®, Cholet, France) was obtained from a local retail store. The proportion of lean meat and fat was determined on the basis of information on the package. Ground beef was provided in vacuum-packed portions of 100 g. The samples were quickly frozen in a -20 °C freezer (Servathin, Carrières-sous-Poissy, France) and stored in a freezing chamber at -20 ± 1 °C. Before each experiment, a bag of the sample was thawed for 18 h in a cooling chamber (4 °C).

2.1.2 Preparation of bacteria inoculum

The strain of *Escherichia coli* K12 (CIP 54.117, N° 11.612) used in this study was provided by the Pasteur Institute, France, in the form of a freeze-dried sample. The strain was rehydrated in 0.2 mL and inoculated in 5 mL of Brain Heart Infusion (BHI) (Panreac Applichem – Darmstadt, Germany) at 37 °C for 18 h at 150 rpm (Incubator Shaker Series – Model Excella E24, New Jersey, USA). A pre-culture was prepared with 0.1 mL of the preceding suspension and inoculated in blood agar (Columbia + 5% Sheep blood - Bio-Rad -

Marnes-la-Coquette, France) at 37 °C, for 18 h. A clone of the pre-culture was then dissolved in 2 mL of sterile water (0.85% NaCl - Medium, BioMerieux). 0.1 mL of this solution was isolated in several Petri dishes of the blood agar with a sterile Pasteur pipette and incubated under the same conditions. The colonies of this second isolation were removed with a sterile swab and dissolved in 1 mL of the beef serum (Eurobio Serum Bovin, France) supplemented with 20% (v/v) glycerol and stored frozen at -80 °C (Thermo Scientific TSE - USA).

To reactivate the strain, 0.1 mL of the stocked culture was inoculated into the blood agar (Columbia agar + 5% sheep blood – 43041, BioMérieux, France) and incubated at 37 °C for 18 h. Fresh colonies were carefully removed with a sterile swab and dissolved in 5 mL of medium suspension (Api 20150, BioMérieux, France) until a cellular concentration of 0.5 McFarland was reached (Densitometer Densimat, BioMérieux, Italy). The optical density of 0.5 McFarland standard is comparable to that of a bacterial suspension concentration of approximately 1.5 x 10^8 CFU/mL (CLSI, 2012).

2.1.3 Inoculation of ground beef

Raw ground beef samples (36 g) were removed aseptically from their refrigerated packaging (7 °C) and transferred into sterile polypropylene sampling pouches with 4 g of bacterial suspension. Ground beef was mixed manually to evenly distribute the inoculum throughout the sample, producing an initial cell concentration of approximately 10^7 CFU/g. For heat treatment, 3 g of inoculated ground beef samples were aseptically placed in packaging of 11.6 mm wide x 60 mm long.

2.1.4 Heat treatment for microbial inactivation

As illustrated in Figure 1, each sample was inserted into the cylindrical vessel and submitted to a linear heating ramp in a programmable Peltier-based effect water bath (Hart Scientific AOIP, FC 9105, USA). After the heating treatment, the sample was quickly cooled to 20 °C by ice immersion. The temperature was measured with a thermocouple (type-K) positioned near the bottom of the sample. The data were collected by a data logger (AOIP Datalog, 91133 Ris Orangis, France) with output recordings every 1 second. To obtain the inactivation kinetics curves, eight final temperatures (50, 52, 54, 56, 58, 60, 62 and 64 °C) were considered. Six different heating rates (1, 3, 5, 7, 10 and 13 °C/min) were applied. Triplicates were carried out for each experiment.

118 *2.1.5 Microbial enumeration and expression of results*

119 The method of analysis was according to ISO 16649-1 (2001). This standard procedure
120 specifies a horizontal method for the enumeration of β-glucuronidase-positive *Escherichia*
121 *coli* in products intended for human consumption. It is based on a colony-count technique at
122 44 °C in a solid medium containing a chromogenic ingredient for detection of the β-
123 glucuronidase enzyme (ISO 16649-1, 2001).

124 Untreated inoculated ground beef and treated ground beef were aseptically removed from the
125 packaging and transferred to a sterile filtered stomacher bag (400 mL, BagPage, St. Nom,
126 France). The samples were diluted with 1:9 (w/w) of buffered peptone water (BK131HA,
127 Biokar Diagnostics, France) and stomached for 2 min at 230 rpm (Stomacher Lab Blender
128 InterscienceBagMixer® - 400, Grosseron, St. Herblain, France). Decimal serial dilutions were
129 performed in buffered peptone water. 1 mL of the initial suspension or decimal dilution was
130 inoculated onto duplicate plates of tryptone-bile-glucuronic (TBX) medium (BK146HA,
131 Biokar Diagnostics, France) and incubated between 18 h to 24 h at 44 °C. The presence of
132 blue colonies is considered to be β-glucuronidase-positive *Escherichia coli*.

133 Each dish containing less than 150 typical CFU was numbered and the result was calculated
134 as the arithmetic mean from two parallel plates. The results expressed to the base 10
135 logarithm of the microbial population for each temperature measurement were collected. The
136 detection limit was fixed to 1 CFU/g of the ground beef.

137 ***2.2 Model design section***

138 *2.2.1 Heat transfer and computational fluid dynamics (CFD)*

139 The experimental methodology described in section 2.1.4 was considered in a CFD-heat
140 transfer model, with the following assumptions:

141 - *Assumption 1:* Water in the cylindrical vessel and the packaged sample were at the
142 same initial homogeneous temperature (7 °C).
143 - *Assumption 2*: The ground beef sample was considered as being homogeneous and
144 isotropic.
145 - *Assumption 3*: Specific heat, density and thermal conductivity of the ground beef were
146 considered as being constant within the temperature range (Pan & Paul Singh, 2001;
147 Tsai, Unklesbay, Unklesbay, & Clarke, 1998).

- *Assumption 4*: The geometry of the packaged sample was an ellipsoid-cylinder and the cross-section was considered homogeneous along the z-coordinate.
- *Assumption 5:* Axial symmetry was supposed for both thermal problems and fluid mechanics, limiting the size to one quarter of the experimental apparatus.
- *Assumption* 6: The mass transfer and the shrinkage of the sample were assumed to be negligible (in-package thermal treatment).
- *Assumption 7:* The package thickness was sufficiently thin to neglect its impact on the heat transfer (low thermal resistance).

The model is aimed at predicting the temperature profile when a heating rate is applied to the wall of the water bath heating cell. The model consists of two main computational domains: the first relates to liquid water which partially fills the cylindrical cell, the second is the ground beef sample located at the centre of the cell. As illustrated in Figure 2, the sample was immersed in water and its upper surface was exposed to air surrounding the medium (natural convection). The lateral surfaces of the cylinder are modelled with a first type boundary condition ($T = T_{cylinder\ cell}$).

2.2.2 Heat transfer modelling

Heat transfer is based on the general heat equation, which depends on thermophysical properties. For the ground beef sample, the heat equation is reduced to:

$$\rho_{(sample)}\, C_{p\,(sample)} \frac{\partial T}{\partial t} = div\,(\lambda_{(sample)}\, \nabla T) \tag{1}$$

For liquid water, a convective term is added to take into account the variation of the thermophysical properties of water as a function of temperature:

$$\rho_{(water)}\, C_{p\,(water)} \frac{\partial T}{\partial t} + \rho_{(water)}\, C_{p\,(water)}\, \vec{u} \nabla T = div\,(\lambda_{(water)}\, \nabla T) \tag{2}$$

Where $\vec{u}$ is the velocity field at any point of the 3D sample domain (u, v, w components). The initial and boundary conditions are defined with the following mathematical expressions:

$$T = T_0, \quad t = 0, \quad \forall (x, y, z), \quad T_0 = 7°C \tag{3}$$

$$\lambda_{(sample\,/\,water)} \left.\frac{\partial T}{\partial z}\right|_{z=L} = h_{air}(T - T_\infty), \quad \forall (x, y,), \forall t > 0, \quad T_\infty = 20°C \tag{4}$$

The boundary condition expressed by equation 4 is applied to the upper surface of water and sample.

$$T_{cylindrical\ cell} = T_0 + \frac{dT}{dt}\,t \quad \begin{cases} for\ \ (x,y) \in [0;R]\ and\ Z = 0, \quad \forall t > 0 \\ for\ \ x, y = R, \quad \forall t > 0, \ \ for\ \ Z \in \ [0, L] \end{cases} \tag{5}$$

Figure 2 displays the coordinate system used to describe these mathematical expressions.

The convective heat transfer coefficient is due to natural convection between the surrounding air medium and the upper surface of the product. Free convection occurs only at the upper surface of both the water and the sample (Figure 2). An empirical correlation was conducted to compute the heat transfer coefficient on the upper cooled side of the cylinder. The air heat transfer coefficient (h_{air}) at the surface of the vertical cylinder with its axis running vertically is the same as that from a vertical plate, so long as the thermal boundary layer is thin (Churchill & Chu, 1975).

2.2.3 Fluid flow modelling

The fluid flow is due to natural convection occurring within the liquid water. This convective flow is modelled from the Navier Stokes equations (Newtonian fluid with incompressible flow). Both the continuity and momentum equations are described as follows:

$$\begin{cases} \dfrac{\partial u}{\partial x} + \dfrac{\partial v}{\partial y} + \dfrac{\partial w}{\partial z} = 0 \qquad\qquad (continuity) \\ \rho_{water}\ \dfrac{d\vec{u}}{dt} = \rho_{water} g - \nabla P + \mu_{water} \Delta\vec{u} \quad (momentum) \end{cases} \tag{6}$$

with

$$\frac{d\vec{u}}{dt} = \frac{\partial \vec{u}}{\partial t} + \left(\vec{u}\,\nabla\right)\vec{u} \tag{7}$$

The associated initial and boundary conditions are given as:

$$P = P_{atm} + \rho_{water}\ g\ z \quad at \quad t = 0, \forall x, y, \quad for\ z \in [0; L] \tag{8}$$

$$\vec{u} = 0 \quad at \quad R = x, y, \quad \forall t > 0, \quad for\ z \in [0; L] \tag{9}$$

For validation purposes, coupled heat transfer and fluid flow were solved for a heating rate of 10 °C /min to compare the simulation to experimental results in the same conditions.

2.2.4 Thermophysical properties

Thermophysical properties of the sample used for modelling purposes are listed in Table 1. The apparent specific heat (C_p) of ground beef (5% fat) was determined using a differential scanning calorimetry (μDSC VII Evo - Setaram Instrumentations, France) at a constant pressure. Samples (~ 500 mg) were weighed in aluminium cells and sealed. A hermetically sealed empty cell was used as a reference. The samples were equilibrated at 20 °C and then heated to 65 °C, at a heating rate of 1 °C/min. The measurements were made in triplicate and the average values were determined.

The density and the thermal conductivity of sample were taken from Pan & Paul Singh (2001). The authors reported densities of 1006-1033 kg/m^3 and thermal conductivities of 0.35-0.41 W m^{-1} °C^{-1} of ground beef (4.8% fat). These values do not change significantly as a function of temperature range (between 5 and 75 °C).

Thermophysical properties of water were considered as temperature dependent (Green & Perry, 2007). These properties were directly implemented in the model using polynomial interpolation functions (Table 2).

2.2.5 Computational details for CFD simulations

Based on the finite element method, the model solved the partial differential equations numerically, with the computational code COMSOL® Multiphysics 5.3a. In this study, the geometry consisted of irregular shapes (ellipsoid-cylinder with axial symmetry) justifying the use of the finite element method to simulate the coupled CFD-heat transfer phenomenon.

As shown in Figure 3, the generated mesh was designed for a 3D configuration, to ensure good accuracy for the numerical resolution (522 830 tetrahedral elements with appropriate boundary layers at the near-cell wall zone). Additional mesh sensitivity studies were performed to obtain accurate number of mesh elements in relation to the computational cost. The mesh independency to the numerical results was also verified. First, the fluid flow was solved as a stationary study in order to initialize the velocity field for a better consistent initial value.

Due to the temperature-dependent thermophysical properties of water, the coupled equations (Eq. 6 and 7) within fluid and heat transfer within the meat sample (Eq. 1) and water (Eq. 2) were solved as a time-dependent study with a direct solver (strong coupling). To ensure a good consistent initial value, the initial time step for the resolution was fixed at 10^{-7} s. Based on these computational details, the computational time did not exceed 4 hours 9 minutes and 12 seconds on a Dell® Precision TM Workstation computer, equipped with 2×Intel® Xeon processors (8 cores), at 2.5 GHz, with 256 GB of RAM, running on Windows®8 Professional, 64 bits.

Several simulations were performed depending on the heating rate being tested (from 1 to 13 °C/min).

2.2.6 Microbial inactivation model

The dynamic non log-linear model developed by Geeraerd et al. (2000) was selected in this study. The reduced model, without the tailing effect, consists of two coupled ordinary differential equations as follows:

$$\frac{dN}{dt} = -k_{\max}\left(\frac{1}{1+C_c}\right)N \tag{10}$$

$$\frac{dC_c}{dt} = -k_{\max}C_c \tag{11}$$

where N represents the microbial cell density (CFU/g). In equation 10, $\frac{dN}{dt}$ is forced to zero once the limit of detection (1 CFU/g) is reached. k_{max} denotes the specific inactivation rate (s^{-1}) and C_c is related to the physiological state of cells (-). A single value for $C_c(0)$ can be used for all experiments, since the methodology of inoculation is standardized. Consequently, a similar initial physiological state is expected for cells

The temperature effect on kinetic parameters (k_{max}) was expressed using Bigelow's (1921) equation:

$$k_{\max}(T) = \frac{\ln 10}{D_{ref}}\exp\left(\frac{\ln 10}{z}\left(T - T_{ref}\right)\right) \tag{12}$$

where D_{ref} denotes the decimal reduction time (s) at the reference temperature T_{ref} and z-value the thermal resistance constant (°C).

2.2.7 *Parameter estimation procedure*

The approach consists in estimating the model parameters of Equation 12 by minimizing the residual sum of squares (RSS):

$$RSS = \sum_{i=1}^{n} \left(l \log \frac{\frac{1}{v}\int N_{simu}(t_i)\, dv}{N_0} - \log \frac{\overline{N}_{exp}(t_i)}{N_0} \right)^2 \quad (13)$$

where t_i are the times at which the thermocouple located in the sample reached the expected the temperatures (respectively 50, 52, 54, 56, 58, 60, 62 and 64 °C), n is the number of experimental data points, N_{simu} is the volume-averaged value of the simulated cell density at t_i. N_{exp} is the volume-averaged value of the triplicate experimental cell density at t_i. V is the volume of the sample and N_0 is the initial cell density.

To minimize the RSS, the Levenberg-Marquardt algorithm (*lsqnonlin* available in Matlab®7.10) was used. This algorithm is based on the least-squares minimization technique and is an improvement of the Gauss-Newton algorithm. In addition, confidence intervals at 95% were calculated for the estimated parameters using *nlparci* function available in Matlab®7.10.

2.2.8 *Methodology used for model comparison and selection*

Considering the model proposed by Geeraerd et al. (2000), it appears that parameters $C_c(0)$, D_{ref} and z-value can be estimated to fit the experimental data. Nevertheless, it is necessary to evaluate the relevance of the number of adjusted parameters. In this contribution, a non-linear least squares approach based on minimization of the RSS (residual sum of squares) is used. It evaluates the well-known Akaike Information Criterion (AIC) (Akaike, 1974), which provides a means for model selection. AIC is established as follows, on the assumption that the residues distribution is Gaussian:

$$AIC = 2\ p - 2 \ln (LL) \quad (14)$$

Where p is number of independently adjusted parameters within the model and LL is the maximum likelihood. If the AIC criterion is used only with the aim of comparing models, the following simplified expression is used:

$$AIC^{*} = 2\ p + \frac{RSS}{\sigma^{2}} \quad (15)$$

When the residual sum of squares are almost equal for two different models, the minimum AIC estimation selects the model with the lowest number of parameters according to the "principle of parsimony" (Yamaoka, Nakagawa, & Uno, 1978). In addition, a variance σ^2 was calculated for each heating rate from the experimental results obtained in triplicate.

3. Results and discussion

3.1 Specific heat of ground beef

The apparent specific heat (C_p) of ground beef at 5% fat was determined from 20 to 65 °C. As can be observed in Figure 4, the C_p values were found to be quite constant on the temperature range. The average measured value ($C_p = 3.69 \pm 0.01$ kJ kg^{-1} K^{-1}) is close to the reported one in the literature for meat product (Zhang, Lyng, Brunton, Morgan, & McKenna, 2004). The C_p average value was integrated directly into the heat transfer model.

3.2 Heat transfer and CFD model validation

To validate the modelling approach, the experimental temperatures measured as a function of time in both the water and the sample were compared to the one simulated from the CFD-heat transfer model. Figure 5 illustrates the case for a heat treatment at 10 °C/min. The standard deviation of the experimental data was about ± 0.3 °C, corresponding to the measuring accuracy of the thermocouple used. Figure 5 depicts the linear setting temperature. The agreement between experimental and model temperatures of the water and the sample is noticeable. Non-negligible thermal delays (about 26 s and 57 s) can be observed respectively between the water and the sample and the set temperature and the sample, justifying the interest of such an approach when heating rates are applied.

The CFD modelling enabled prediction of the velocity fields due to the natural convection problem within a static enclosure. The Navier-Stokes equation was solved by considering a laminar flow. The norm of the velocity field, for example at 10 °C/min, is depicted in Figure 6

for different processing times. Fluid motion occurs (illustrated by black arrows in Figure 6), because of the temperature dependent thermophysical properties of water. Recirculation of the heating fluid leads to velocity gradients, with a maximum value of 2.5 mm/s around the sample (norm of the velocity field). The Reynold number was calculated considering this maximum fluid velocity of 10 °C/min with a value of 9.4. This result clearly demonstrates a natural convection of water within a confined space, in which the flow regime is laminar.

Once the CFD approach is validated, the model illustrates the temperature gradients when heating rates are applied. Figure 7 illustrates the temperatures at the final time of simulation for the six different heating rates considered. Simulation was stopped when the simulated temperature of the corresponding point to the thermocouple position reached 64 °C.

For all treatments the hottest zone was located at the surface of the sample, except for the upper central part, due to contact with ambient air (cooling). The coldest zone was along the central axis of the product. The temperature gap between the hottest and coldest zones increased with the applied heating rates, so 4.3, 6.2, 8.1, 9.8, 12.4, and 15.8 °C for 1, 3, 5, 7, 10 and 13 °C/min, respectively.

To confirm the effect of temperature heterogeneities on the volumetric microbial inactivation, equations 10, 11 and 12 were used. The simulation of the 3D local temperature distribution in the meat sample (CFD and heat transfer model solved by COMSOL® and transposed to MATLAB®) was performed to quantify the 3D local microbial inactivation. For example, under a thermal treatment at 10 °C/min, the numerical result illustrated a thermal cartography with hot and cold points. These temperature heterogeneities lead to heterogeneous local microbial inactivation represented by the hatched area in Figure 8.

In Figure 8, a total inactivation can be seen for the hottest point after 5.8 minutes. For the coldest point, the maximum inactivation achieved was of 2 Log_{10}, at the end of treatment. However, it is not possible to experimentally validate these local microbial inactivation data, at every geometrical point of the domain. Consequently, the use of a mathematical model to describe the local microbial inactivation during a pasteurization process remains a relevant tool. More, it confirms the importance of considering the volumetric distribution of temperature in the meat product to accurately predict microbial inactivation.

3.3 Estimation of kinetic parameters of inactivation

Various results can be found in the literature concerning evaluation of kinetic parameters (D_{ref}, T_{ref} and z-value) under isothermal conditions. In a study of heat resistance of *Escherichia coli* 0157:H7 inoculated into 7% fat ground beef, Ahmed et al. (1995) obtained a D_{ref}, by linear regression, of 684 s (at 55 °C) and 27 s (at 60 °C), and a z-value equal to 4.78 °C. In the same strain, but in ground beef with 4.8% fat, Smith et al. (2001) calculated by first-order kinetics a D_{ref} equal to 73 s (at 58 °C) and 19 s (at 61 °C), for a z-value of 3.79 °C. These variations might be attributed to differences in the strains of *E. coli* used, the fat content of meat, along with differences in recovery methods and sample size (Smith et al., 2001; Stringer, George, & Peck, 2000). In both studies, the values of D_{ref} differ greatly whereas z-value remains in the same order of magnitude.

In this study, ground beef with 5% fat was used and the heating rates described above were applied. Despite these dynamical conditions, in a first approach, the parameters D_{ref} = 73 s, z-value = 3.79 °C and T_{ref} = 58 °C obtained by Smith et al. (2001) in isothermal conditions and $C_c(0)$ = 0.23, as reported in Hamoud-Agha et al. (2013), were used in the Geeraerd et al. (2000) model. Results are illustrated in Figure 9. Black circles illustrate the experimental data in triplicate, whereas the predictions obtained using the aforementioned parameters are represented by broken blue lines. Note that the model underestimates the experimental inactivations, but this underestimation has the same order of magnitude whatever the heating rate.

A second approach consisted in estimating the model parameters from the dynamic experiments. First, the triplet parameters $C_c(0)$, D_{ref} and z-value were estimated. Poschet et al., (2005) showed that the uncertainties on D_{ref} and z-value are minimal when T_{ref} is equal to the middle of the lethal experimental temperature range. As D_{ref} is closely linked to T_{ref}, this value was fixed at 58 °C, as defined in Smith et al. (2001). The $C_c(0)$ value was estimated with a lower bound equal to zero. In table 3, $C_c(0)$ is not significantly different from zero for all heating rates. Consequently, equation (11) can be removed and the Geeraerd et al. (2000) model becomes a classical first order inactivation model.

With the Bigelow model, the D_{ref} and z-values were estimated (Table 4). It should be noted that these AIC^* values are lower than the AIC^* values obtained in previous estimate procedure with three parameters (Table 3). The confidence intervals for D_{ref} increase for extreme heating rates (10 and 13 °C/min), certainly due to the large thermal heterogeneities. Another

explanation is based on Van Derlinden, Balsa-Canto, & Van Impe, (2012), where the authors discussed the link between parameter identifiability and the shape of the temperature profile. The results of z-value indicated in Table 4 are consistent with those presented by Smith et al. (2001), for a similar product at 58 °C (z-value = 3.79 °C). Indeed, this value (3.79 °C) is almost included in the confidence intervals and will thus be considered hereafter.

With the estimation limited to D_{ref}, the confidence intervals are widely reduced, even if they remain significant for heating rates of 10 and 13 °C /min (12.52 s and 8.75 s). These results are summarized in Table 5. Compared to Table 4, quite similar or lower values of the AIC* were obtained. It appears that adjusting D_{ref} is sufficient to fit the experiments without degrading the AIC* values. Moreover, it also reduces the parameter uncertainties as verified with 95% confidence intervals.

Thereby, for one estimated parameter, the D_{ref} values remain in the same order of magnitude. Consequently, the average of the previously estimated D_{ref} values (Table 5) of 47 s was used. The predicted inactivation curves obtained in this case are presented in black continuous line in Figure 9. They are very close to inactivation results obtained with each estimated D_{ref} (red dotted line is superimposed on black continuous line in figure 9). Hence, for D_{ref} values ranging from 40 to 50 s, considering a unique value of 47 s does not significantly affect the inactivation predictions.

Finally, results reveal that the k_{max} expression with temperature dependence proposed by Bigelow is sufficient to fit experimental data obtained in dynamic conditions with large temperature heterogeneities (>15 °C for 13 °C /min), provided that these heterogeneities are considered in the prediction model. Constant values for T_{ref}, z and D_{ref} can be considered for all heating rates in the range 1 to 13 °C /min. Additionally, T_{ref} and z-values of literature (Smith et al., 2001) were used with only a fitting of D_{ref}.

4. Conclusion

The contribution of this work lies in the integration of experimental and numerical approaches dedicated to the real-food pasteurization process including both thermal and inactivation kinetics with high heating rates.

The originality of this paper lies (*i*) in the integration of three-dimensional heat transfer conditions in parameter estimations applied to the inactivation model and (*ii*) in the application of extreme heating rates to challenge the validity of the Geeraerd modelling

393 approach developed for isothermal conditions. The heat transfer model was validated during
394 blank tests, and the volume-average of logarithmic inactivation was considered to be
395 comparable with experimental data. In addition, the experiments were carried out on real
396 ground beef, and not in capillary tubes, as usually proposed. The inactivation model was
397 coupled with heat transfer to design a 3D simulator to predict the spatial distribution of
398 logarithmic inactivation of *E. coli* in a meat sample.

399 Such a 3D simulator illustrates how the temperature gradients can provoke large inactivation
400 heterogeneities, and thus the necessity to consider them in realistic pasteurization conditions.
401 The satisfactory agreement between model and experiments allows coupling of the modelling
402 approach with process control procedures, allowing energy supply to reach the expected
403 microbial inactivation while limiting temperature heterogeneities. Such an objective could be
404 reached for example by using combined energy sources with volumetric heating to avoid
405 overtreatment at the surface of the food product (microwaves, ohmic heating).

406 **Acknowledgments**

407 The authors are grateful to the National Council for Scientific and Technological
408 Development (CNPq, Brazil) for C. D. Albuquerque's PhD scholarship and financial support
409 (process number 232767/2014-9).

410 **References**

411 Ahmed, N. M., Conner, D. E., & Huffman, D. L. (1995). Heat-resistance of Escherichia Coli
412 O157:H7 in meat and poultry as affected by product composition. *Journal of Food*
413 *Science*, *60*(3), 606–610.
414 Akaike, H. (1974). A New Look at the Statistical Model Identification. *IEEE Transactions on*
415 *Automatic Control*, *19*(6), 716–723.
416 Bhuvaneswari, E., & Anandharamakrishnan, C. (2014). Heat transfer analysis of
417 pasteurization of bottled beer in a tunnel pasteurizer using computational fluid dynamics.
418 *Innovative Food Science and Emerging Technologies*, *23*, 156–163.
419 Bigelow, W. D. (1921). The logarithmic nature of thermal death time curves. *The Journal of*
420 *Infectious Diseases*, *29*(5), 528–536.
421 Boillereaux, L., Curet, S., Hamoud-Agha, M., & Simonin, H. (2013). Model-based settings of
422 a conveyorized microwave oven for minced beef simultaneous cooking and
423 pasteurization. In *Computer Applications in Biotechnology (CAB 2013)*. Mumbai, India.

Bott, R. (2014). *Modelling microorganisms in food*. (S. Brul, Suzanne van Gerwen, & M. Zwietering, Eds.), *Woodhead Publishing Limited, Abington Hall, Abington*. Cambridge.

Chen, G. (2013). Estimating microbial survival parameters from dynamic survival data using Microsoft Excel. *International Journal of Food Science and Technology*, *48*(9), 1841–1846.

Chung, H. J., Wang, S., & Tang, J. (2007). Influence of heat transfer with tube methods on measured thermal inactivation parameters for Escherichia coli. *Journal of Food Protection*, *70*(4), 851–859.

Churchill, S. W., & Chu, H. H. S. (1975). Correlating equations for laminar and turbulent free convection from a vertical plate. *International Journal of Heat and Mass Transfer*, *18*(11), 1323–1329.

Cordioli, M., Rinaldi, M., Copelli, G., Casoli, P., & Barbanti, D. (2014). Computational fluid dynamics (CFD) modelling and experimental validation of thermal processing of canned fruit salad in glass jar. *Journal of Food Engineering*, *150*, 62–69.

Denys, S., Pieters, J. G., & Dewettinck, K. (2003). Combined CFD and experimental approach for determination of the surface heat transfer of the surface heat transfer coefficient during thermal processing of eggs. *Journal of Food Science*, *68*(3).

Dimou, A., & Yanniotis, S. (2011). 3D numerical simulation of asparagus sterilization in a still can using computational fluid dynamics. *Journal of Food Engineering*, *104*(3), 394–403.

Franklin R. Cockerill, III, MD Matthew A. Wikler, MD, MBA, FIDSA Jeff Alder, PhD Michael N. Dudley, PharmD, FIDSA George M. Eliopoulos, MD Mary Jane Ferraro, PhD, MPH Dwight J. Hardy, PhD David W. Hecht, M., & Janet A. Hindler, MCLS, MT(ASCP) Jean B. Patel, PhD, D(ABMM) Mair Powell, MD, FRCP, FRCPath Jana M. Swenson, MMSc Richard B. Thomson, Jr., PhD Maria M. Traczewski, BS, MT(ASCP) John D. Turnidge, MD Melvin P. Weinstein, MD Barbara L. Zimmer, P. (2012). Methods for Dilution Antimicrobial Susceptibility Tests for Bacteria That Grow Aerobically ; Approved Standard — Ninth Edition. In *Clinical and Laboratory Standards Institute Advancing* (Vol. 32, p. 88).

Garre, A., Huertas, J. P., González-Tejedor, G. A., Fernández, P. S., Egea, J. A., Palop, A., & Esnoz, A. (2018). Mathematical quantification of the induced stress resistance of microbial populations during non-isothermal stresses. *International Journal of Food Microbiology*, *266*(September 2017), 133–141.

Geeraerd, A. H., Herremans, C. H., & Van Impe, J. F. (2000). Structural model requirements

458 to describe microbial inactivation during a mild heat treatment. *International Journal of*
459 *Food Microbiology*, *59*(3), 185–209.
460 Green, D. W., & Perry, R. H. (2007). *Perry's Chemical Engineering Handbook* (Eighth). The
461 McGraw-Hill Companies, Inc.
462 Hamoud-Agha, M. M., Curet, S., Simonin, H., & Boillereaux, L. (2013). Microwave
463 inactivation of Escherichia coli K12 CIP 54.117 in a gel medium: experimental and
464 numerical study. *Journal of Food Engineering*, *116*(2), 315–323.
465 Hassani, M., Cebrián, G., Mañas, P., Condón, S., & Pagán, R. (2006). Induced
466 thermotolerance under nonisothermal treatments of a heat sensitive and a resistant strain
467 of Staphylococcus aureus in media of different pH. *Letters in Applied Microbiology*,
468 *43*(6), 619–624.
469 ISO 16649-1:2001.Microbiology of food and animal feeding stuffs - Horizontal method for
470 the enumeration of beta-glucuronidase-positive Escherichia coli - Part 1: Colony-count
471 technique at 44 degrees C using membranes and 5-bromo-4-chloro-3-indolyl. (2001).
472 Juneja, V. K., & Marks, H. M. (2003). Characterizing asymptotic D -values for *Salmonella*
473 spp . subjected to different heating rates in sous-vide cooked beef, *4*, 395–402.
474 Marcotte, M., Chen, C. R., Grabowski, S., Ramaswamy, H. S., & Piette, J. P. G. (2008).
475 Modelling of cooking-cooling processes for meat and poultry products. *International*
476 *Journal of Food Science and Technology*, *43*(4), 673–684.
477 Marquardt, D. W. (1963). An algorithm for least-squares estimation of nonlinear parameters.
478 *Journal of the Society for Industrial and Applied Mathematics*.
479 Pan, Z., & Paul Singh, R. (2001). Physical and thermal properties of ground beef during
480 cooking. *LWT - Food Science and Technology*, *34*(7), 437–444.
481 Poschet, F., Geeraerd, A. H., Loey, A. M. Van, Hendrickx, M. E., & Impe, J. F. Van. (2005).
482 Assessing the optimal experiment setup for first order kinetic studies by Monte Carlo
483 analysis, *16*, 873–882.
484 Smith, S. E., Maurer, J. L., Orta-Ramirez, A., Ryser, E. T., & Smith, D. M. (2001). Thermal
485 inactivation of *Salmonella* spp., *Salmonella typhimurium* DT104 , and *Escherichia coli*
486 O157 : H7 in ground beef. *Food Microbiology and Safety Thermal*, *66*(8), 1164–1168.
487 Stratakos, A. C., & Koidis, A. (2015). Suitability, efficiency and microbiological safety of
488 novel physical technologies for the processing of ready-to-eat meals, meats and
489 pumpable products. *International Journal of Food Science and Technology*, *50*(6), 1283–
490 1302.
491 Stringer, S. C., George, S. M., & Peck, M. W. (2000). Thermal inactivation of Escherichia

492 coli 0157 : H7. *Joumal of Applied Microbiology Symposium Supplement*, *88*(Coia 1998),
493 79S–89S.
494 Tsai, S. J., Unklesbay, N., Unklesbay, K., & Clarke, A. (1998). Thermal properties of
495 restructured beef products at different isothermal temperatures. *Journal of Food Science*,
496 *63*(3), 481–484.
497 Valdramidis, V. P., Belaubre, N., Zuniga, R., Foster, A. M., Havet, M., Geeraerd, A. H., …
498 Kondjoyan, A. (2005). Development of predictive modelling approaches for surface
499 temperature and associated microbiological inactivation during hot dry air
500 decontamination. *International Journal of Food Microbiology*, *100*(1–3), 261–274.
501 Valdramidis, V. P., Geeraerd, A. H., Bernaerts, K., & Van Impe, J. F. (2006). Microbial
502 dynamics versus mathematical model dynamics: The case of microbial heat resistance
503 induction. *Innovative Food Science and Emerging Technologies*, *7*(1–2), 80–87.
504 Valdramidis, V. P., Geeraerd, A. H., & Impe, J. F. Van. (2007). Stress-adaptive responses by
505 heat under the microscope of predictive microbiology. *Journal of Applied Microbiology*,
506 *1*, 1922–1930.
507 Van Derlinden, E., Balsa-Canto, E., & Van Impe, J. F. M. (2012). (Optimal) experiment
508 design for microbial inactivation. In Progress on quantitative approaches of thermal food
509 processing. In Vasilis P. Valdramidis & Jan F. M. Van Impe (Eds.), *Progress on*
510 *Quantitative Approaches of Thermal Food Processing* (pp. 67–98). Nova Publishers.
511 Vilas, C., Arias-Méndez, A., García, M. R., Alonso, A. A., & Balsa-Canto, E. (2018). Toward
512 predictive food process models: A protocol for parameter estimation. *Critical Reviews in*
513 *Food Science and Nutrition*, *58*(3), 436–449.
514 Yamaoka, K., Nakagawa, T., & Uno, T. (1978). Application of Akaike's information criterion
515 (AIC) in the evaluation of linear pharmacokinetic equations. *Journal of*
516 *Pharmacokinetics and Biopharmaceutics*, *6*(2), 165–175.
517 Zhang, L., Lyng, J. G., Brunton, N., Morgan, D., & McKenna, B. (2004). Dielectric and
518 thermophysical properties of meat batters over a temperature range of 5–85 °C. *Meat*
519 *Science*, *68*(2), 173–184.
520

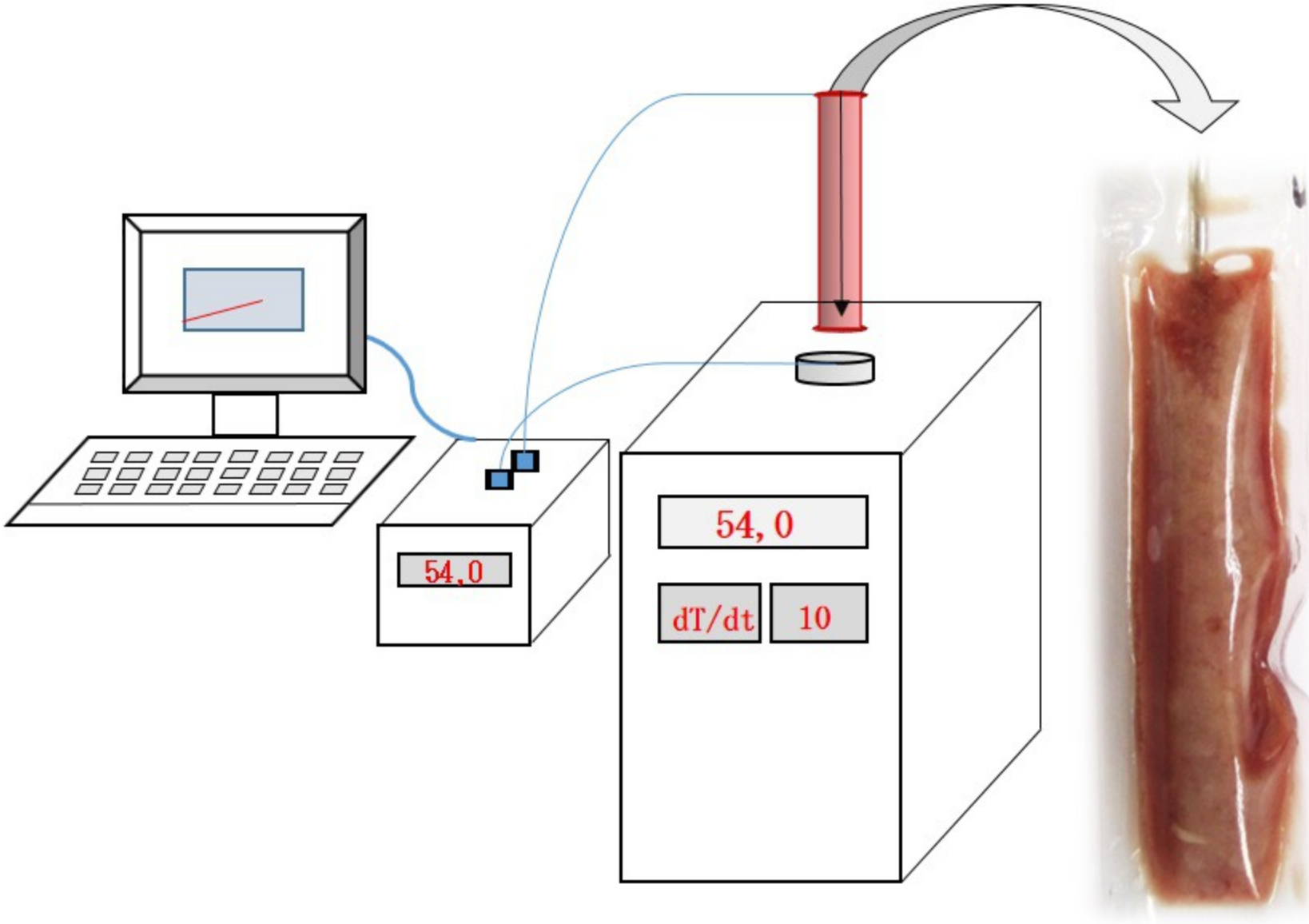
54.0
54, 0
dT/dt
10

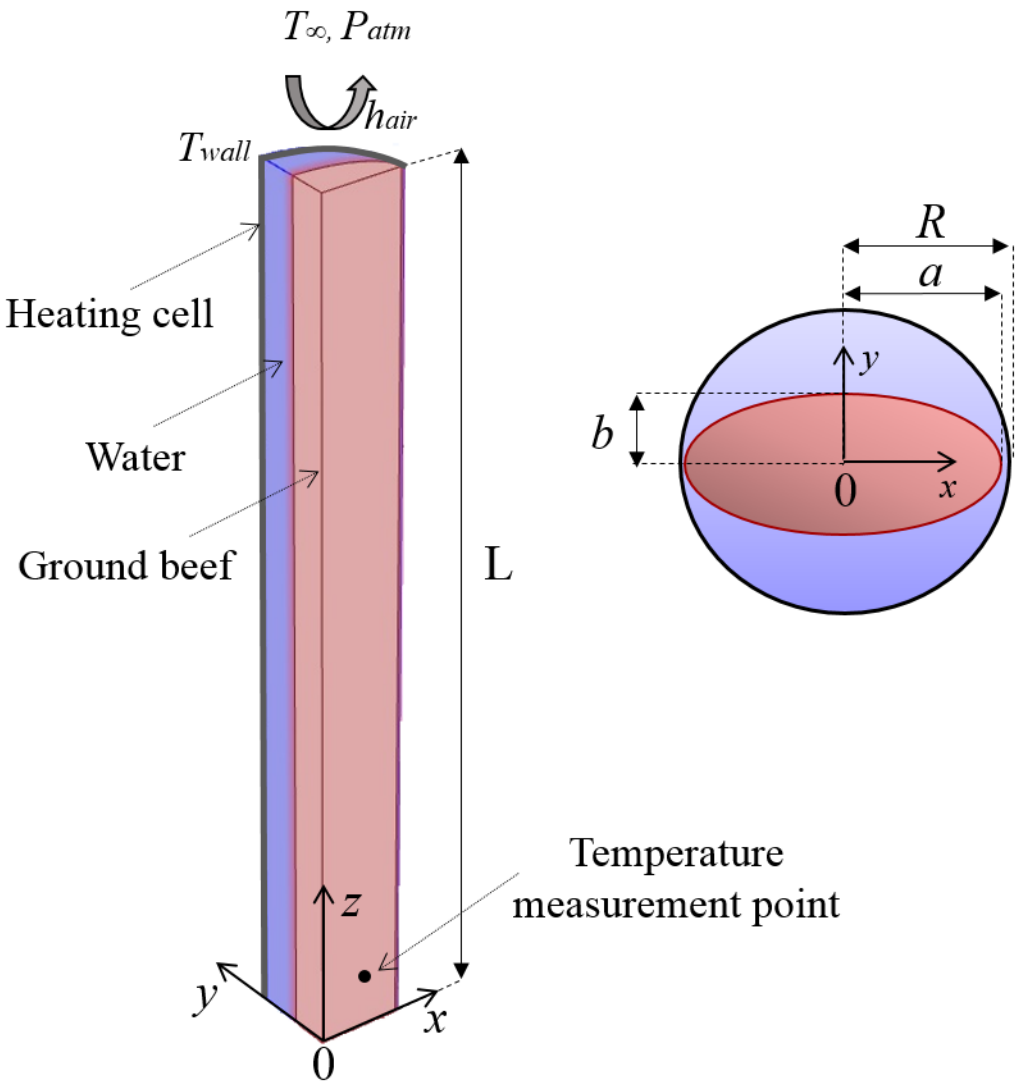
T_∞, P_{atm}
h_{air}
T_{wall}
Heating cell
Water
Ground beef
L
R
a
b
y
0
x
z
y
x
0
Temperature
measurement point

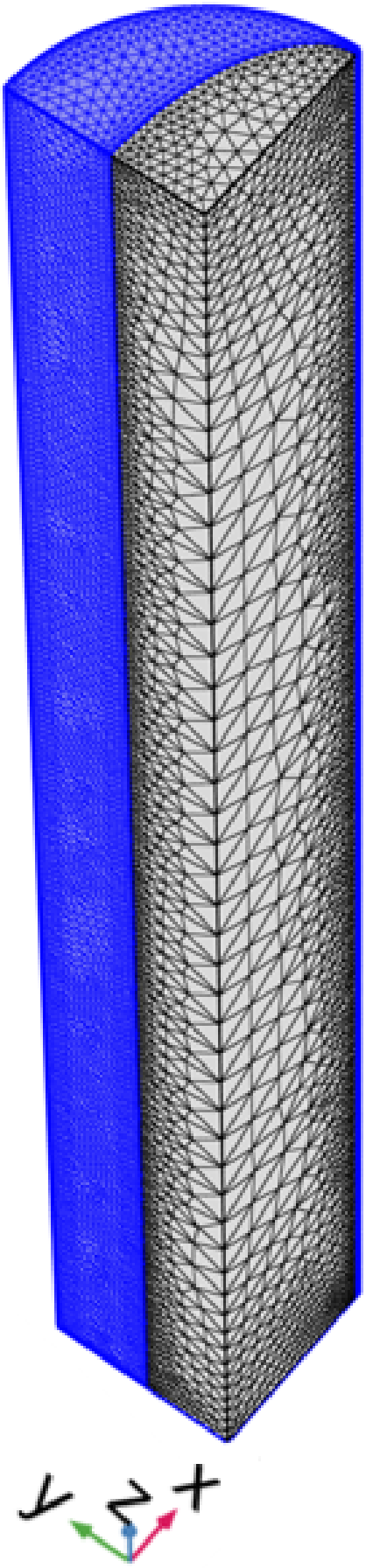
Y
Z
X

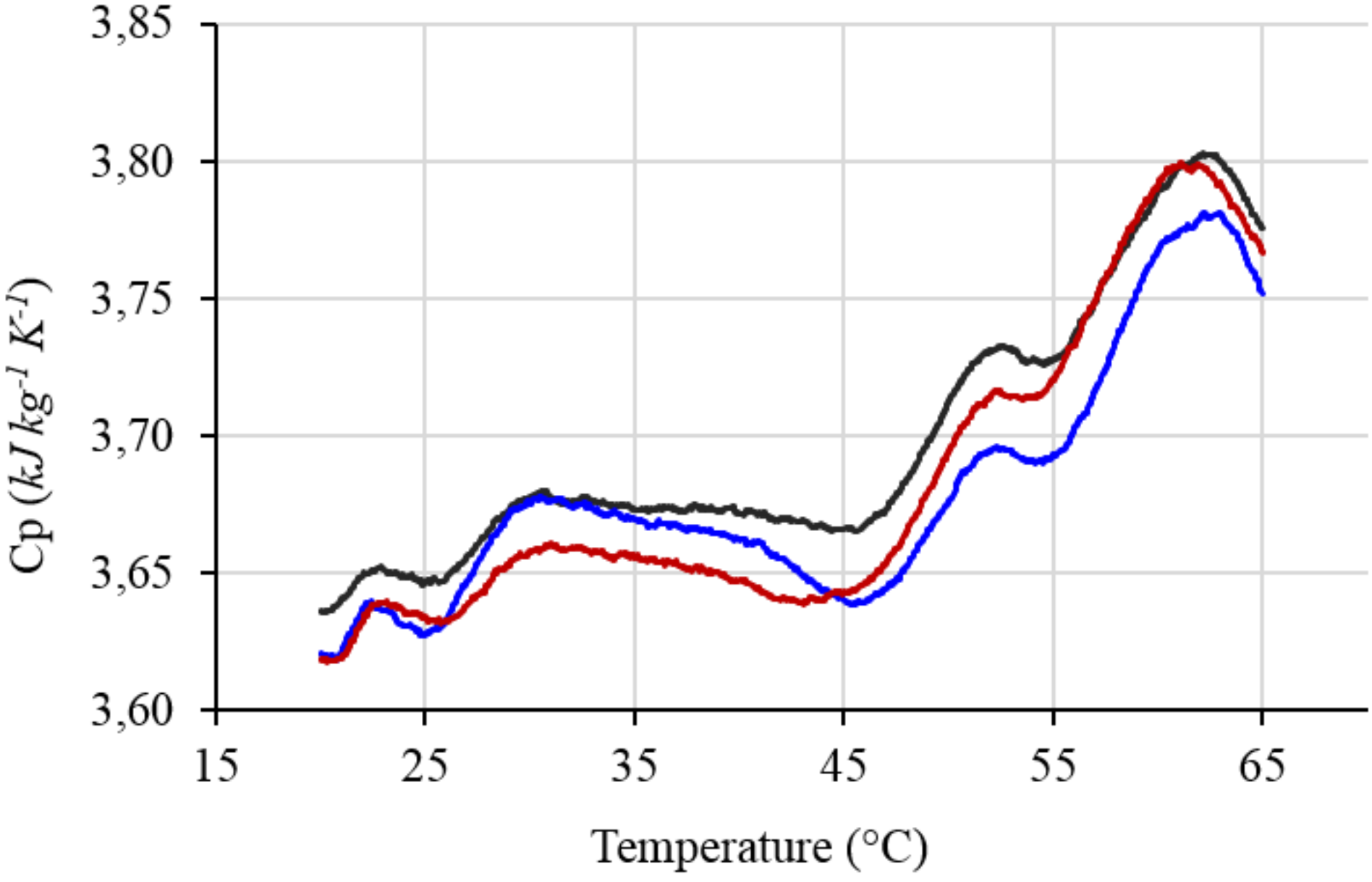
3,85
3,80
3,75
3,70
3,65
3,60
Cp (kJ kg-1 K-1)
15
25
35
45
55
65
Temperature (°C)

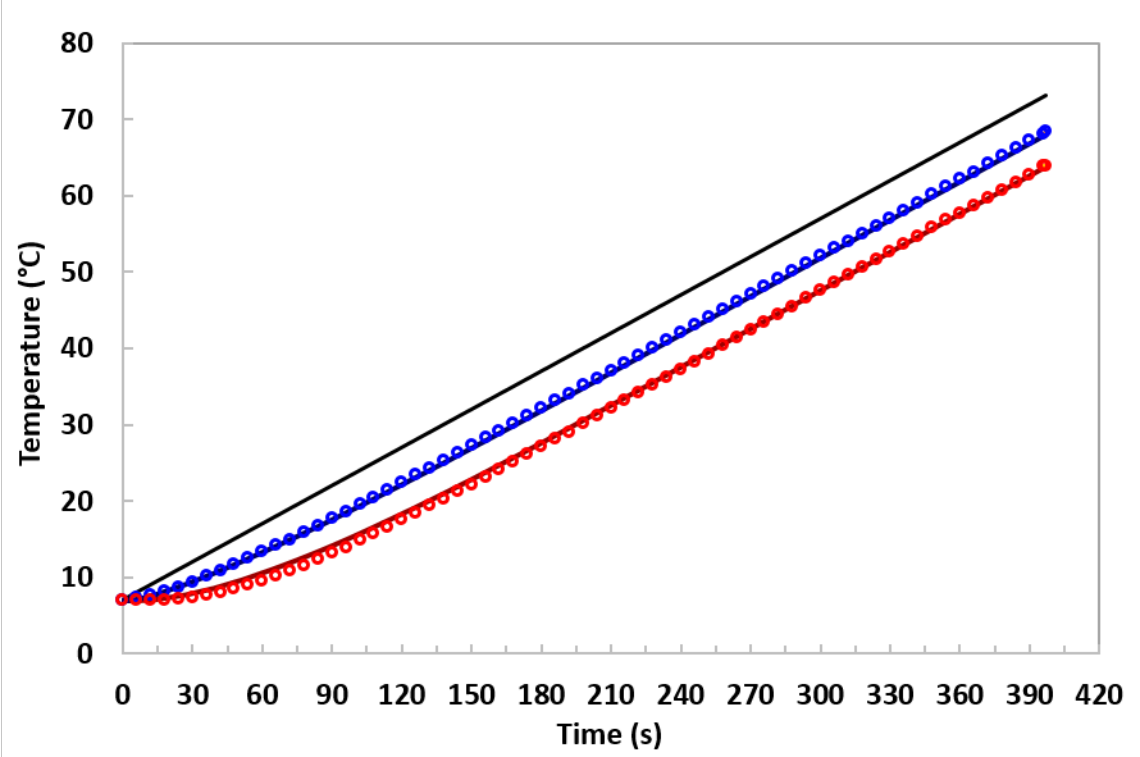
80
70
60
50
40
30
20
10
0
Temperature (°C)
0
30
60
90
120
150
180
210
240
270
300
330
360
390
420
Time (s)

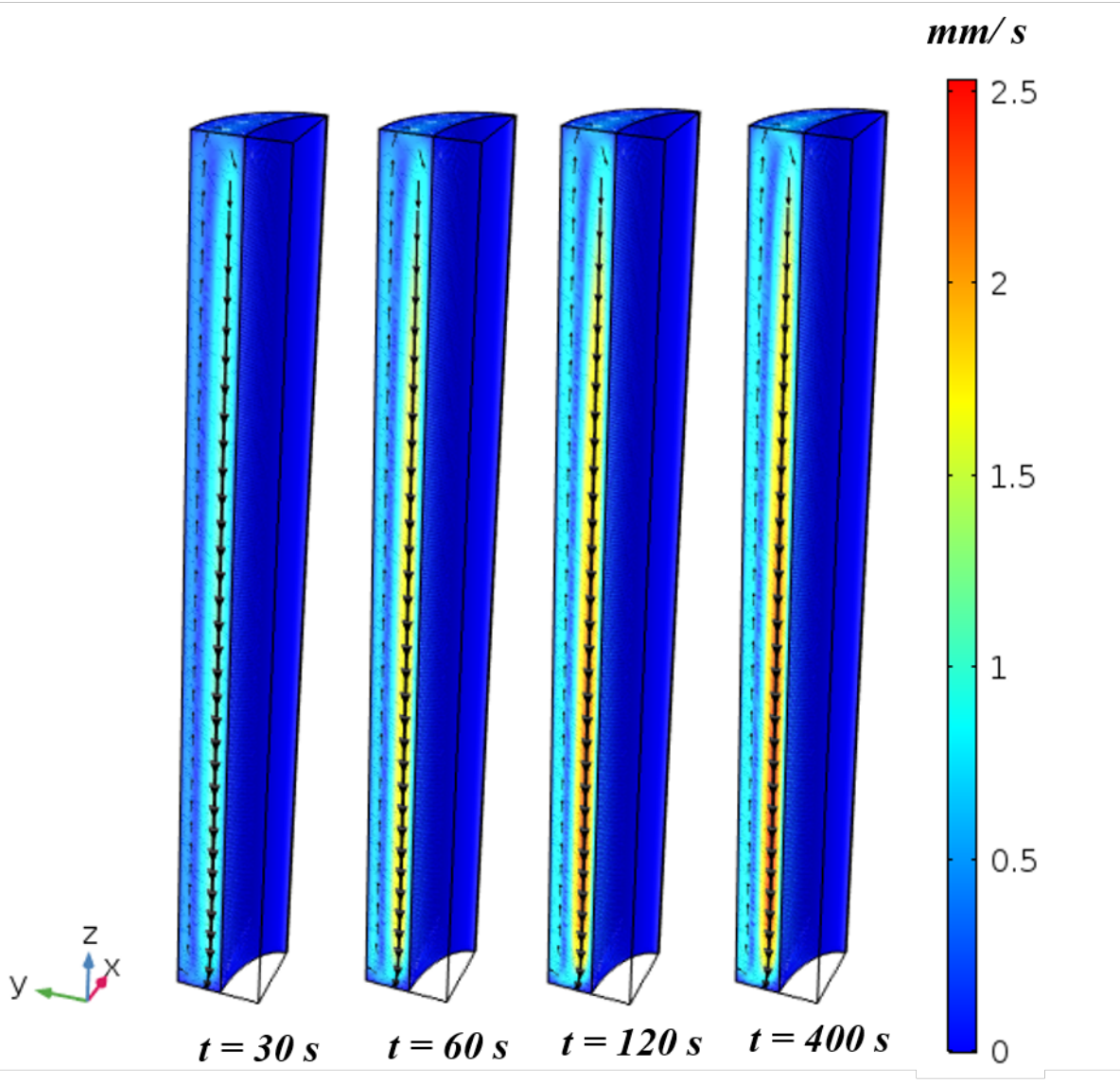
mm/ s
2.5
2
1.5
1
0.5
0
z
x
y
t = 30 s
t = 60 s
t = 120 s
t = 400 s

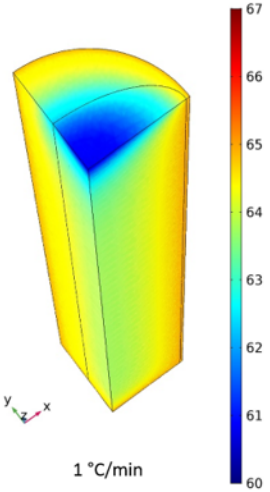

1 °C/min

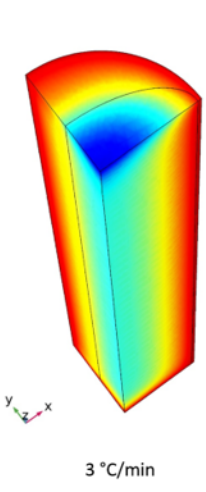

3 °C/min

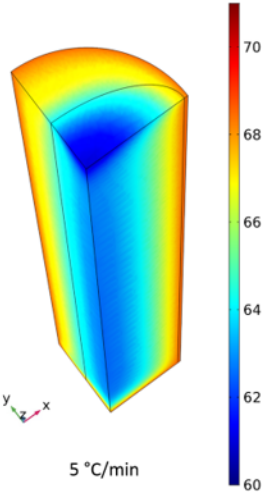

5 °C/min

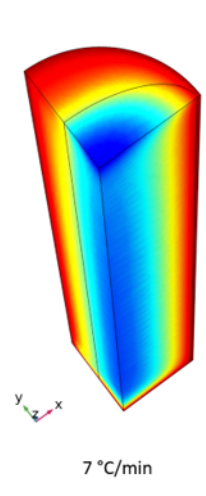

7 °C/min

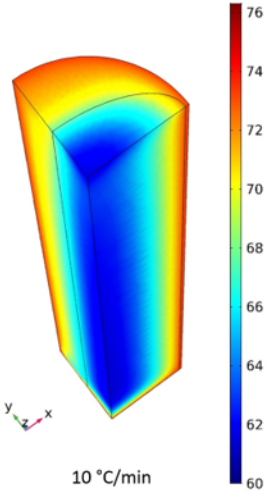

10 °C/min

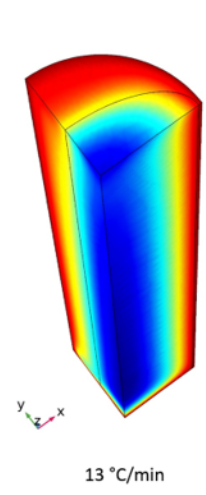

13 °C/min

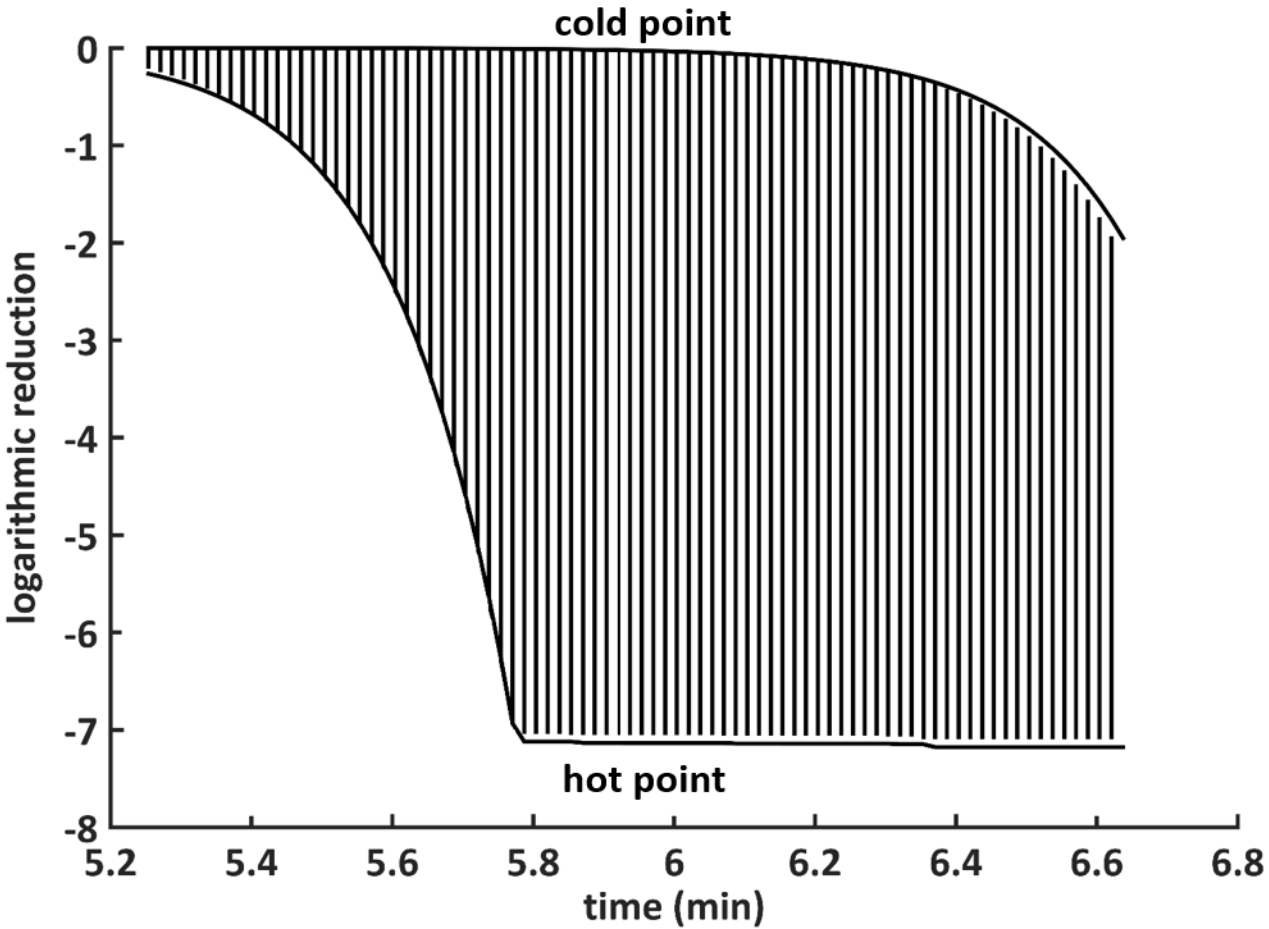
cold point
hot point
logarithmic reduction
time (min)
0
-1
-2
-3
-4
-5
-6
-7
-8
5.2
5.4
5.6
5.8
6
6.2
6.4
6.6
6.8

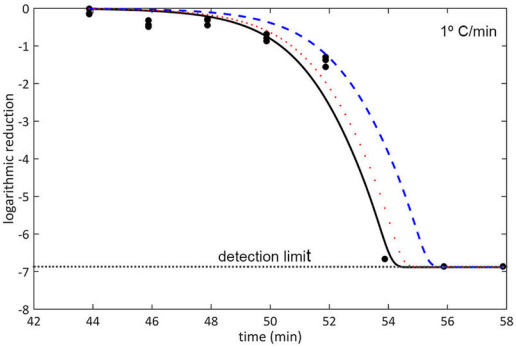
1° C/min
logarithmic reduction
detection limit
time (min)

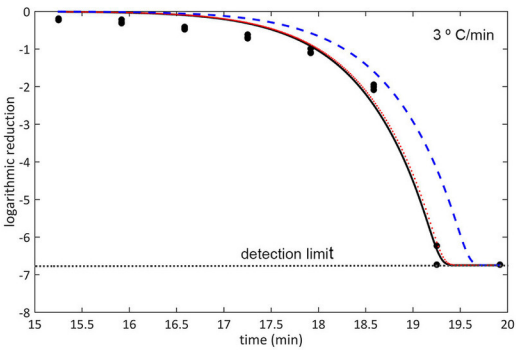
3 ° C/min
logarithmic reduction
detection limit
time (min)

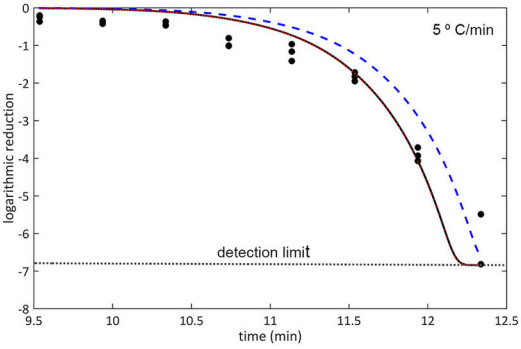
5 ° C/min
logarithmic reduction
detection limit
time (min)

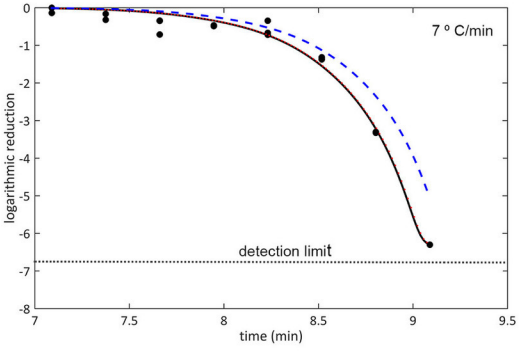
7 ° C/min
logarithmic reduction
detection limit
time (min)

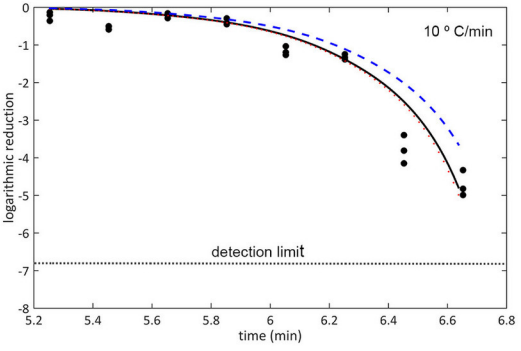
10 ° C/min
logarithmic reduction
detection limit
time (min)

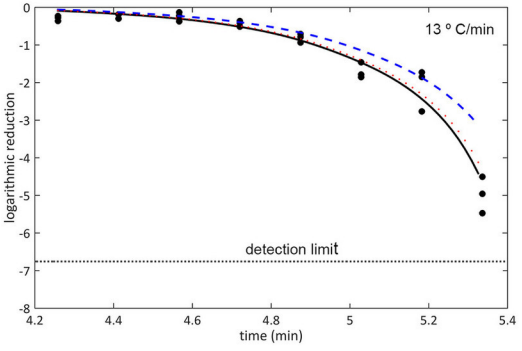
13 ° C/min
logarithmic reduction
detection limit
time (min)

Table 1. Thermophysical properties of ground beef.

Properties	Value	Unit	Source
Apparent specific heat (C_p)	3.69 ± 0.01	kJ kg^{-1} K^{-1}	Experimental
Thermal conductivity (λ)	0.35	W m^{-1} °C^{-1}	Pan and Singh (2001).
Density (ρ)	1006	kg/m^3	Pan and Singh (2001).

Table 2. Thermophysical properties of water as a function of temperature (Kelvin).

Functions of the properties*	Unit
$C_p = 12010.15 - 80.41 \times T + 0.31 \times T^2 - 5.38 \times 10^{-4} \times T^3 + 3.62 \times 10^{-7} \times T^4$	J kg^{-1} K^{-1}
$\lambda = -0.87 + 8.95 \times 10^{-3} \times T - 1.58 \times 10^{-5} \times T^2 + 7.97 \times 10^{-9} \times T^3$	W m^{-1} °K^{-1}
$\rho = 838.47 + 1.40 \times T - 3.01 \times 10^{-3} \times T^2 + 3.72 \times 10^{-7} \times T^3$	kg /m^3

*Green & Perry, 2007

Table 3. Estimated values of D_{ref}, z-value and $C_c(0)$, for T_{ref} = *58 °C.* Standard deviation of experimental data (σ^2), 95% confidence intervals (CI) and simplified Akaike Information Criterion (AIC*).

Heating rate (°C /min)	σ^2	D_{ref} (s)	CI D_{ref}	z-value (°C)	CI z-value	$C_c(0)$	CI $C_c(0)$	AIC*
1	0.24	33.1	3.8	1.96	1.41	0	0.30	11.8
3	0.20	48.9	6.8	3.81	0.63	0	0.21	12.2
5	0.23	41.7	5.3	7.32	1.53	0.11	0.15	10.2
7	0.34	45.7	8.1	3.59	0.61	0.21	0.18	9.3
10	0.50	56.2	22.4	6.19	2.3	0.08	0.17	11
13	0.63	74.7	33.1	2.99	0.69	0.04	0.15	9.2

Table 4. Estimated values of D_{ref} and z-value (T_{ref} = *58 °C*). Standard deviation of experimental data (σ^2), 95% confidence intervals (CI) and simplified Akaike Information Criterion (AIC*).

Heating rate (°C /min)	σ^2	D_{ref} (s)	CI D_{ref}	z-value (°C)	CI z-value	AIC*
1	0.24	33.1	3.8	1.96	1.41	8.8
3	0.20	48.9	6.8	3.81	0.63	9.2
5	0.23	40.8	5.1	6.70	1.41	7.2
7	0.34	31.4	12.4	4.80	0.81	7.2
10	0.50	62.1	23.2	5.98	2.65	8.2
13	0.63	73.1	32.6	3.02	0.71	6.6

Table 5. Estimated values of D_{ref} (z = 3.79 and T_{ref} = *58* °C). Standard deviation of experimental data (σ^2), 95% confidence intervals (CI) and simplified Akaike Information Criterion (AIC*).

Heating rate (°C/min)	σ^2	D_{ref} (s)	CI D_{ref}	AIC*
1	0.24	40.1	0.03	9
3	0.20	47.5	0.38	6.2
5	0.23	50.0	0.59	8.2
7	0.34	50.0	0.48	3.6
10	0.50	50.1	12.52	6.8
13	0.63	46.7	8.75	3.6